The contribution of luminance and chromatic channels to color assimilation

Xavier Otazu

Computer Vision Center and Computer Science Department, Universitat Autonoma de Barcelona, Barcelona, Spain

Xim Cerda-Company

Computer Vision Center, Vall d'Hebron Research Institute, and Computer Science Department, Universitat Autonoma de Barcelona, Barcelona, Spain

Color induction is the phenomenon where the physical and the perceived colors of an object differ owing to the color distribution and the spatial configuration of the surrounding objects. Previous works studying this phenomenon on the *lsY* MacLeod–Boynton color space, show that color assimilation is present only when the magnocellular pathway (i.e., the *Y* axis) is activated (i.e., when there are luminance differences). Concretely, the authors showed that the effect is mainly induced by the koniocellular pathway (*s* axis), but not by the parvocellular pathway (*l* axis), suggesting that when magnocellular pathway is activated it inhibits the koniocellular pathway. In the present work, we study whether parvo-, konio-, and magnocellular pathways may influence on each other through the color induction effect. Our results show that color assimilation does not depend on a chromatic–chromatic interaction, and that chromatic assimilation is driven by the interaction between luminance and chromatic channels (mainly the magno- and the koniocellular pathways). Our results also show that chromatic induction is greatly decreased when all three visual pathways are simultaneously activated, and that chromatic pathways could influence each other through the magnocellular (luminance) pathway. In addition, we observe that chromatic channels can influence the luminance channel, hence inducing a small brightness induction. All these results show that color induction is a highly complex process where interactions between the several visual pathways are yet unknown and should be studied in greater detail.

Introduction

Color induction is a known phenomenon, exploited by artists for several centuries (Chevreul, 1839; Von Bezold, 1876), and widely studied by researchers (Ehrenstein, 1941; Van Tuijl, 1975; Monnier & Shevell, 2003, 2004; Gordon & Shapley, 2006; Faul et al., 2008; Bimler et al., 2009; Otazu et al., 2010; Kaneko & Murakami, 2012; Cerda-Company et al., 2018). This phenomenon appears when the perceived color of a target is influenced by the surrounding colors. According to the color shift direction, color induction can be distinguished into two types: color contrast and color assimilation. The former occurs when the color of the target shifts away from the color of the nearest surrounding object (the inducer). In contrast, the latter occurs when the color of the target shifts toward that of the inducer. For example, when a gray target is surrounded by a green inducer and it is perceived as reddish (the opponent color of green), color contrast is induced. Instead, if the gray target is perceived as greenish, color assimilation is induced. The type of induction (contrast or assimilation) mainly depends on the spatiochromatic properties of the target and the inducers. Several studies showed that striped surrounds usually induce color assimilation and uniform surrounds usually induce color contrast (Monnier & Shevell, 2003, 2004; Shevell & Monnier, 2005; Otazu et al., 2010).

In a recent study, we observed that luminance differences are a key factor to induce color assimilation in the *s* chromatic axis (Cerda-Company et al., 2018). There, we used striped stimuli that lay down on either the *l* or the *s* chromatic axis of the *lsY* MacLeod-Boynton color space (MacLeod & Boynton, 1979), which is a commonly used opponent color space based on the Smith and Pokorny (1975) cone fundamentals. In this color space, *l* and *s* chromatic axes correspond with the red–green (parvocellular pathway, a.k.a., P pathway) and purple–lime (koniocellular pathway, a.k.a., K pathway) opponent chromatic channels, respectively, and the *Y* axis corresponds with the luminance channel (magnocellular pathway, a.k.a., M pathway). We observed that equiluminant stimuli (no luminance difference between the test and the inducers) did not induce color assimilation, or it was negligible. In addition, we observed that, mainly along

the s chromatic axis, the induced color changed from no induction (or weak contrast) to color assimilation by increasing the luminance difference between the target and the inducer.

Several authors suggested that color induction is the result of the neural mechanisms (probably the lateral connections) in the primary visual cortex (Zaidi et al., 1992; Rossi et al., 1996; De Weert & Kruysbergen, 1997; Zaidi, 1999; Shapley & Hawken, 2002; Cao & Shevell, 2005). In this visual area, there exist three types of cells: single- (SO), double- (DO), and non-opponent (NO) neurons (Johnson et al., 2001; Shapley & Hawken, 2002; Johnson et al., 2008; Shapley & Hawken, 2011). SO neurons, which are also known as *color* cells, respond best to low spatial frequencies ($\nu < 0.5$ cycles/°; i.e., low pass), and chromatic stimuli (color-sensitive cells). DO neurons, which are also called *color-luminance* cells, are band pass (0.5 cycles/° $< \nu < 10$ cycles/°, with the peak of response at 2 cycles/°) and sensitive to both color and luminance borders. NO neurons, which are also called *luminance* cells, are band pass cells and sensitive to achromatic stimuli. Interestingly, it is suggested that DO neurons play a major role in color appearance (Nunez et al., 2018).

One of the proposed neural mechanisms for color induction is the mutual inhibition (Gordon & Shapley, 2006; Xing et al., 2015; Nunez et al., 2018), where as luminance contrast (i.e., the luminance difference) is increased, the color response is decreased by virtue of connections between luminance and color-sensitive cells. That is, NO and DO cells could inhibit DO and SO activity. This mechanism could explain the observed luminance–chromatic interaction in our previous study (Cerda-Company et al., 2018), where color assimilation only appeared when there existed luminance differences. In this previous study, we only evaluated the influence of the M pathway on the P and K chromatic pathways separately. At this point, a new question could arise: Is this mechanism also present between the P and K pathways? An affirmative answer would imply that, when both chromatic pathways are activated, the P pathway inhibits the K pathway and vice versa. Extending our previous work, in the present study, we explored the possibility that mutual inhibition occurs between chromatic pathways (i.e., a chromatic–chromatic K–P interaction), aside from the influence of the M pathway.

The hypothesis of the present study is that chromatic pathways influence each other by a mutual inhibition–like mechanism. Considering the described mutual inhibition mechanism between luminance and chromatic pathways, therefore, we expect to observe color assimilation at equiluminance (when both chromatic pathways are activated), and the maximum color assimilation at non-equiluminance (when all pathways inhibit each other, and the mutual inhibition is maximal).

To test this hypothesis, we extend our previous study (Cerda-Company et al., 2018) using a visual stimuli where both l and s chromatic channels are simultaneously activated. We also study its dependency on the luminance channel (Y axis), to investigate their possible relationship with the luminance–chromatic mutual inhibition mechanism.

Methods

Apparatus

The experiments were conducted in a dark room; that is, all the light in the room was from the monitor's screen, and the walls were black to avoid interreflections. Stimuli were presented on a calibrated 32″ LCD Display++ monitor (Cambridge Research Systems, Ltd.) at 100 Hz, with 1440×1080 pixels resolution, and subtending 22.6×16.95 visual degrees. The stimuli was viewed binocularly (subject's head was not constrained) from a distance of approximately 134 cm. We used the Cambridge Research Systems ViSaGe MKII Stimulus Generator, capable of displaying 14-bit color depth. The monitor was calibrated via the customary software (Cambridge Research Systems, Ltd.) and the Display++ monitor embedded colorimeter. The subject's responses were collected using a Logitec gamepad.

Stimuli

All stimuli were implemented in Matlab (The MathWorks, Inc., Natick, MA), and the video processor was controlled via a Cambridge Research System custom-made toolbox.

As shown in Figure 1, the spatial configuration of the visual stimuli was the same as in Cerda-Company et al. (2018). That is, the test stimulus (presented on the left side of the monitor) was composed of 11 concentric rings of the same width (15.5 arcmin of visual angle), which included the achromatic equal energy white (EEW) test ring ($l = 0.66$ and $s = 0.98$). Similarly, the luminance of the test ring varied according to the luminance condition: The set of luminance differences between the test and the inducer rings was $\Delta Y = [-10, -5, 0, +5, +10]$, cd/m^2, being the inducer rings $Y = 20$ cd/m^2 (see details in Equiluminance measure). Furthermore, the inducer rings (being the first inducer the one adjacent to the test ring) had opponent chromaticities, with the EEW exactly in the middle of both chromatic points. The chromatic values for l and s axes were the same as in Cerda-Company et al. (2018) (e.g., $l = \{0.63, 0.66, 0.69\}$ and $s = \{0.58, 0.98, 1.38\}$), but we defined four new
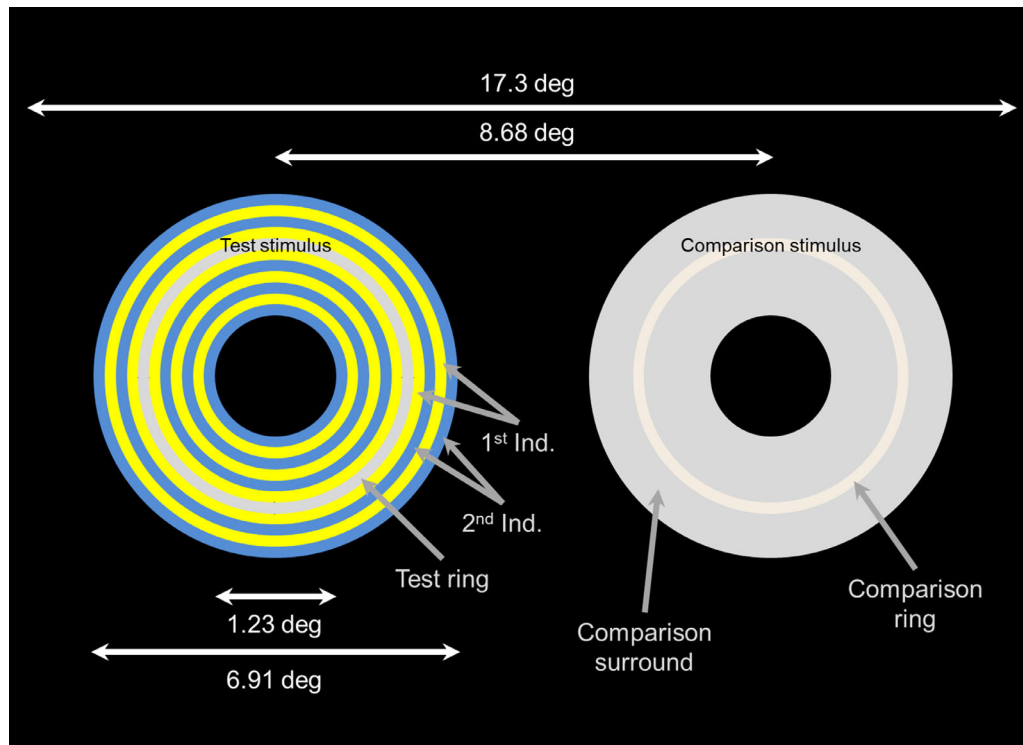
Figure 1. Stimuli design. The first and the second inducers consisted of equiluminant ($Y = 20\,\text{cd/m}^2$) pairs of rings of opposite chromaticities such as RedPurple–GreenLime or PurpleGreen–LimeRed chromaticities. The test ring was always achromatic ($l = 0.66$ and $s = 0.98$) and could have five different luminance values (luminance conditions): $Y = [10, 15, 20\,\text{(equilum.)}, 25, 30]\,\text{cd/m}^2$. Although it is difficult to see in this figure because of their size, 8 black dots of 1 pixel size were drawn around test ring for easier detection: four dots in the inner radius of the ring and four points in the outer radius (at 0°, 90°, 180°, and 270°). Subjects had to match the color of the comparison ring with that of the test ring. Colors in this figure might not be the same as the experiment because they were created for illustrative purposes. Figure extracted from Cerda-Company et al. (2018).

chromatic conditions named as RedPurple–GreenLime, GreenLime–RedPurple, GreenPurple–RedLime, and RedLime–GreenPurple according to their spatial position in the MacLeod–Boynton color space. Their l, s are shown in Table 1. We chose these chromaticities because, in contrast to Cerda-Company et al. (2018), the visual stimuli activate the two chromatic pathways at the same time, which allows us to measure their interaction.

Notation

To name the chromatic values we have used the Cao and Shevell (2005) notation, that is, $-l$ for $l = 0.63$ and $+l$ for $l = 0.69$, and not using any symbol for the $l = 0.66$ case. Similarly, we use $-s$ for $s = 0.58$, $+s$ for $s = 1.38$, and no symbol for $s = 0.98$. The signs refer to whether the value of the chromatic condition is bigger ($+$) or smaller ($-$) than the corresponding value of the achromatic EEW $(l, s) = (0.66, 0.98)$.

To name chromatic conditions, we use the notation of the first inducer (see the Notation column in Table 1). For example, GreenPurple–RedLime condition is denoted as $-l/+s$ (because GreenPurple chromaticity is

Condition	Test ring		First inducer		Second inducer		Notation
	l	*s*	*l*	*s*	*l*	*s*	
Red–Green	0.66	0.98	0.69	0.98	0.63	0.98	*+l*
Green–Red	0.66	0.98	0.63	0.98	0.69	0.98	*−l*
Purple–Lime	0.66	0.98	0.66	1.38	0.66	0.58	*+s*
Lime–Purple	0.66	0.98	0.66	0.58	0.66	1.38	*−s*
RedPurple–GreenLime	0.66	0.98	0.69	1.38	0.63	0.58	*+l/+s*
GreenLime–RedPurple	0.66	0.98	0.63	0.58	0.69	1.38	*−l/−s*
GreenPurple–RedLime	0.66	0.98	0.63	1.38	0.69	0.58	*−l/+s*
RedLime–GreenPurple	0.66	0.98	0.69	0.58	0.63	1.38	*+l/−s*

Table 1. Summary of the experimental conditions. We detail the chromaticity sets in the MacLeod-Boynton color space. Only the *l* and *s* chromatic axes are reported because the luminance of inducers was always $Y = 20\,\text{cd/m}^2$ and the luminance of the test ring depended on the luminance condition: $\Delta Y = [-10, -5, 0\,\text{(equiluminant)}, 5, 10]$. The last column indicates the notation of the inducers (see text). For convention, when two color names (e.g., red–green) are indicated, it means that the first (e.g., red) is the name of the first inducer, and the second name (e.g., green) is the name of the second one. First four conditions (*+l, −l, +s, −s*) are the ones from Cerda-Company et al. (2018).

denoted by $-l/+s$), RedLime–GreenPurple condition as $+l/-s$, and so on.

Results from Cerda-Company et al. (2018) lay on the cardinal axes of MacLeod-Boynton color space, that is, they only activated one chromatic channel (e.g., s or l). Therefore, notation for these points (first four rows in Table 1) is represented by only one letter (e.g., $+l$ for Red–Green, $-l$ for Green–Red, $+s$ for Purple–Lime, and $-s$ for Lime–Purple). In contrast, the results obtained in the present work lie on the diagonal axes of the chromatic plane. Therefore, for these points, the notation is represented by two letters (e.g., $+l/+s$, $+l/-s$, $-l/+s$, $-l/-s$), because both chromatic channels are activated at the same time.

In addition, to name a particular experimental point, we have added the value of the luminance condition (ΔY, the luminance difference between the test and the first inducer) to the end of the previous notation. For example, $+l/-s/0$ refers to the equiluminant ($\Delta Y = 0 \, \text{cd/m}^2$) point for the RedLime–GreenPurple condition, and $+l/-s/5$ refers to the $\Delta Y = 5 \, \text{cd/m}^2$ point of the same chromatic condition.

Equiluminance measure

Because the *equiluminant point* is different for every participant, before the experiment we measured the color values that generated equiluminance. The equiluminant-point measure procedure for every observer lasted 3 hours and was performed through three different days using the minimally distinct border method (MDB) (Boynton & Kaiser, 1968; Kaiser, 1971; Wagner & Boynton, 1972; Boynton, 1973; Kaiser et al., 1990; Brill, 2014). The stimuli consisted on two semicircular adjacent disks presented in the same apparatus as the experiment. One of the disks was achromatic ($l = 0.66$ and $s = 0.98$) and the other had one of the chromaticities defined in the experiment's chromatic conditions (i.e., $+l/+s$, $+l/-s$, $-l/+s$, $-l/-s$) plus an achromatic condition, for control. The luminance of the achromatic disk was set at $Y = 20 \, \text{cd/m}^2$. Subjects task was "to adjust the luminance of the colored disk until the border between the color and the achromatic disks was minimal," that is, when only chromatic but not luminance differences were perceived. Ideally, there would be no border between the two disks (in fact, this should happen for the control condition), but in other conditions, at least a chromatic border was always perceived. We obtained an average (from 8 measures) of the luminance necessary to match each of the four colors to the achromatic disk for each subject. These luminance values were used to construct the inducer rings of the test stimulus (see left stimulus in Figure 1).

Participants

Eleven people recruited from our academic community participated in the experiment. Five were familiar with color spaces (AC, XO, CS, NS, XC) and six were not (RP, YR, YX, AM, HP, SD). Nine of them were completely naïve (AC, RP, YR, CS, NS, YX, AM, HP, SD), and two of them are the authors of this article (XO, XC). The age was between 18 and 48 years old. Six of them were female (RP, YR, CS, NS, YX, HP) and five were male (AC, XO, AM, SD, XC).

All participants had normal or corrected-to-normal vision, and they scored as normals in the Ishiara's test (Ishihara, 1972) and the D-15 Farnsworth Dichotomous Test (Farnsworth, 1947). All of them signed the consent form to participate in the experiment, where the aim of the study was described. The experiment was conducted according to the guidelines of the Declaration of Helsinki, and approved by our university's ethic commitee (Comissio d'Etica en l'Experimentacio Animal i Humana CEEAH-4056 de l'Universitat Autonoma de Barcelona).

To have a similar number of participants in both cardinal and diagonal conditions, three completely naïve participants (CS, DC, MF) performed the experiment described in Cerda-Company et al. (2018). The total number of participants was increased to 10, and their results were added to the previous ones. These participants had normal or corrected-to-normal vision, they were not familiar with colour spaces, their age was between 22 and 24 years of age, and two of them were female (CS, MF) and one was male (DC).

Experimental procedure

After the MDB task to measure the equiluminant colors, participants performed an asymmetric matching task (Figure 1), where they were instructed to "adjust the color of the comparison ring until it was perceived the same as the test ring." To do this matching, participants adjusted independently the chromaticity and the luminance of the comparison ring, navigating in the MacLeod–Boynton color space using the gamepad buttons (Monnier & Shevell, 2003; Cerda-Company et al., 2018). They did a first training session to familiarize with the experimental procedure and the apparatus. All the data collected during this training session was removed from the analyses.

After the training session, participants did five sessions during three different days. Each session lasted 40 minutes (approximately) and they consisted of 3 minutes of darkness adaptation and two trials. Each trial included all possible random combinations of chromatic and luminance conditions ($+l/+s$, $+l/-s$, $-l/+s$, $-l/-s$) $\times$ (-10, -5, 0, 5, 10) cd/m^2, totalling 20

runs each. In a single day, a participant came to the laboratory and spend 90 minutes approximately to do 80 runs (two sessions). Between sessions, participants were forced to take a 10-minute break. After the 5 sessions, the participant finished the 10 trials, totalling 200 runs (matches).

Statistical analysis

To measure the strength of color induction, we used the color induction metric defined in Cerda-Company et al. (2018):

$$\Delta C_i = \frac{C_i^c - C_i^t}{C_i^f - C_i^t}, \quad (1)$$

where $i = [l, s]$, C_i^c was the chromaticity of the comparison ring along the considered color axis, and C_i^t and C_i^f were the chromaticities of the test ring and the first inducer ring along the same axis, respectively. This metric allowed us to capture the two color induction effects: negative values ($\Delta C_i < -JND$) for color contrast and positive values ($\Delta C_i > +JND$) for color assimilation. The just noticeable difference (JND) is the region where no color differences were perceived. We estimated the JND value from CIELab color space ($\Delta E = 1$) because it is an approximately perceptually uniform color space, and then transformed to the MacLeod–Boynton color space.

All statistical analyses were done in R Core Team (2019). Our dependent variable was the color induction strength and, to study its predictors, we fitted Linear Mixed-Effects Models using the function *lmer* from the packages *lme4* and *lmerTest*. Experimental factors such as luminance (ConditionY = [−10, −5, 0, 5, 10]) and chromatic conditions (ConditionL = [−*l*, 0*l*, +*l*] and ConditionS = [−*s*, 0*s*, +*s*]) were considered as fixed factors, and the participants and trials were considered as random factors. In fact, because each participant did 10 trials, the factor trial was nested in participant.

To avoid model over-parametrization, we compared the models with and without each factor using the Akaike Information criterion (AIC) and the likelihood ratio test. Significance levels were calculated using the Kenward–Roger degrees of freedom approximation to the F distribution (Kenward & Roger, 1997). Furthermore, we used the *t* test comparisons to identify the levels with significant differences, when necessary. The *p* values were corrected using the false discovery rate (function *emmeans* from package *emmeans*). Apart from the corrected *p* value (p_{adj}), from the post hoc analysis, we reported the *t*-ratio also.

As a theoretical interpretation of the analyses, a statistically significant interaction between chromatic conditions, would imply that the color induction is explained by the interaction of the two chromatic pathways (P and K). This process would help us to reject or accept our initial hypothesis.

To compare distributions against the zero-value, we used a *t* test for normally-distributed data, and the Mann–Whitney *U* test for data that did not follow a normal distribution (functions *t.test* and *wilcox.test* from package *stats*). From these distributions, we reported the mean value ± the standard deviation for normal-distributed data, or the median and the interdquartile range (in brackets) for non-normally distribute data. Furthermore, we also used these tests to compare two different distributions. From both tests, we reported the *p* values, the *t* values from the *t* test, and the $V-$ or $W-$ values from the Mann–Whitney *U* test. The normal distribution was assessed using the Shapiro–Francia test (function *sf.test* from package *nortest*).

Results

To have an overview of the results, in Figures 2 and 3, we show the color induction strength obtained in the present study together with the extended results from Cerda-Company et al. (2018) (+*l*, −*l*, +*s*, −*s*). Each panel represents a single chromatic condition (see Table 1) and, in them, the color induction along the *l*, the *s*, and the *Y* axes is shown (red, purple, and black lines, respectively). Because some chromatic conditions are defined on the cardinal axes (+*l*, −*l*, +*s*, −*s*), the color induction metric cannot be measured along the other axis. Instead, the effect can be measured on both axes for the chromatic conditions defined on the diagonals (+*l*/+*s*, +*l*/−*s*, −*l*/+*s*, −*l*/−*s*). Results in the MacLeod–Boynton color space and all individual results for each chromatic conditions are shown in Appendixes A and B, respectively.

According to the metric (Equation 1), we can observe that, on one hand, several conditions induced color assimilation (e.g., +*s*/<0 and −*s*/>0). On the other hand, several conditions induced color contrast (e.g., −*l*/<0 and −*l*/−*s*/<0). Moreover, because several values are not above the JND, we can observe conditions where no color induction was induced (e.g., +*l*/0 and +*l*/−*s*/0).

In agreement with previous studies (Fach & Sharpe, 1986; Cerda-Company et al., 2018; Cerda-Company & Otazu, 2019), we observed that color induction along the two chromatic axes depends on both the chromatic and luminance conditions. This observation is supported by the best fitted linear model: ColorInduction$_{l,s}$ ∼ ConditionL * ConditionS * ConditionY + (1|Participant). We fit a specific linear model for each chromatic axis, being the
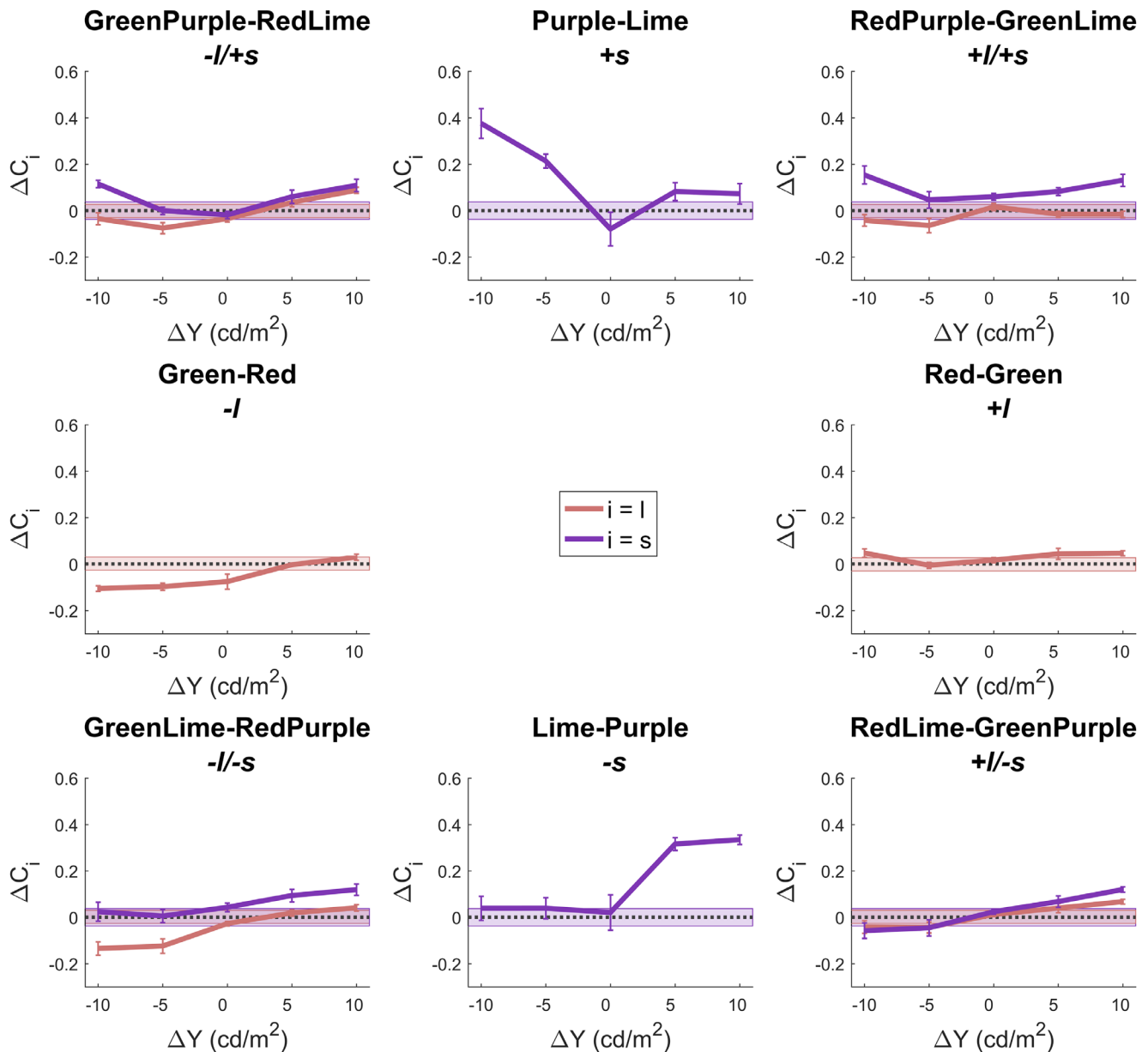
Figure 2. Results on the cardinal axis (e.g., *+l*, *−l*, *+s*, *−s*,) are extended from Cerda-Company et al. (2018), and results on the diagonal axis (e.g., *+l/+s*, *+l/−s*, *−l/+s*, *−l/−s*) have been obtained in the present study. For the sake of clarity, chromatic conditions (panels) are spatially distributed similarly to their position with respect to the EEW in the chromatic plane of the MacLeod–Boynton color space. Error bars are standard error of means. ΔY is the luminance condition (the luminance difference between the test and the first inducer), ΔC_i is the color induction metric (positive values mean assimilation and negative values mean contrast). Red and purple lines are results for *l* and *s* axes, respectively. The JND values are shown as a coloured area, for example, transparent red for *l* and transparent purple for *s*.

$AIC_l = -818.40$ and $AIC_s = -463.34$. The random factor (participant) explained the 16.8% of the variability of data that is not explained by the fixed factors along the *l* axis, and the 18.0% along the *s* axis. Interestingly, we did not include the trials as a random factor because the model became singular, that is, this factor made the model more complex, but did not improve it. Therefore, all the observations were averaged for each participant and condition. All details about these models are reported in Appendix C.

The two fitted models are similar in the sense that both show significant interactions between all chromatic and luminance channels. Indeed, along the *l* axis, we observe a main effect of ConditionL ($F(1, 265.91) = 33.12$, $p < .0001$) and ConditionY ($F(4, 265.76) = 39.56$, $p < .0001$), indicating that
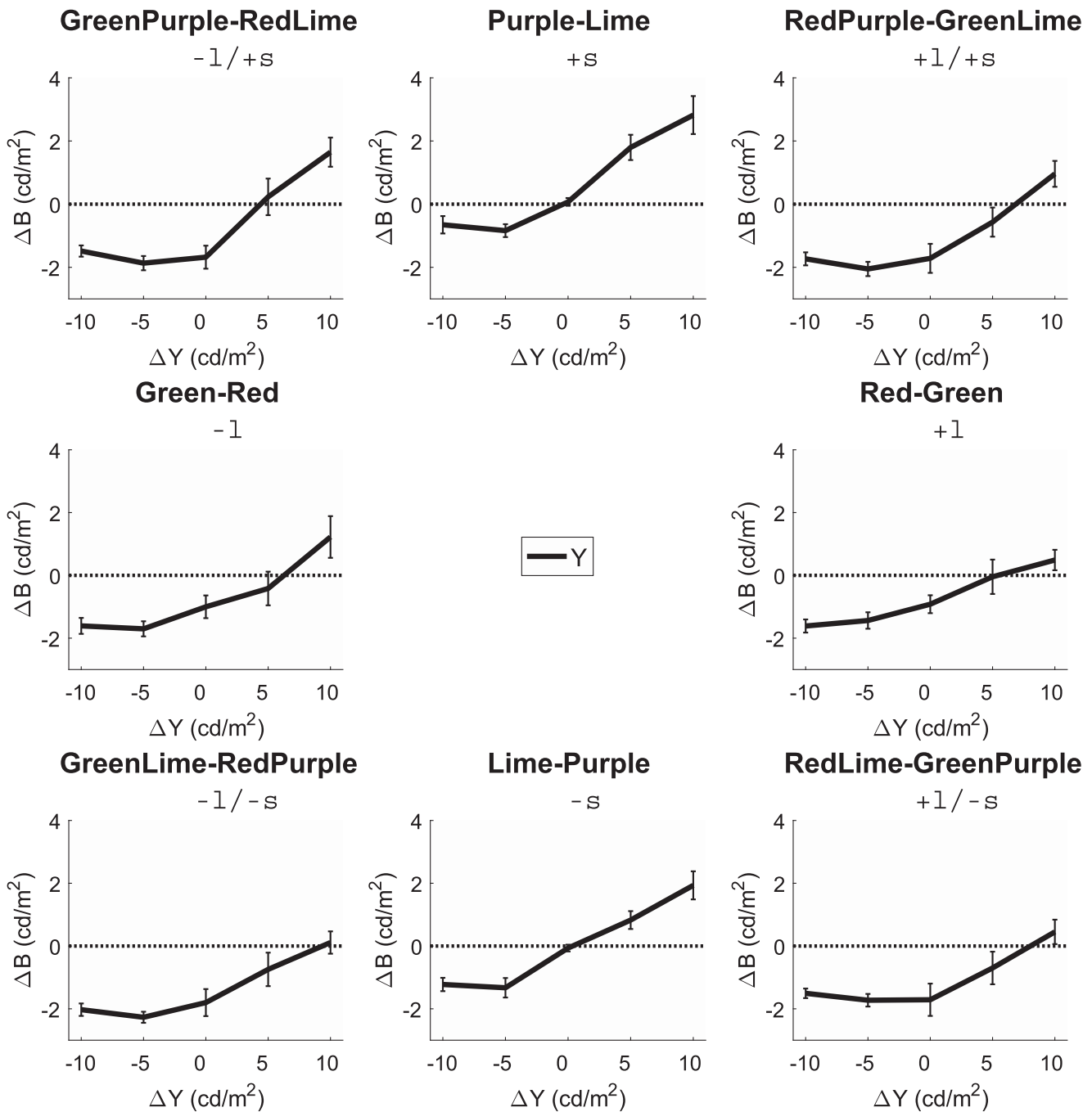
Figure 3. Brightness induction estimation, that is, luminance difference between the comparison and the test rings (ΔB), for every condition. Error bars are standard error of the means. Positive values $\Delta B > 0$ means that the test ring was perceived brighter than its luminance, and negative values $\Delta B < 0$ indicate that it was perceived darker. For $\Delta B = 0$, the luminance of the test and the comparison rings are equal, that is, no brightness induction. In this figure, we can observe that a chromatic surround induces brightness contrast (i.e., $\Delta B \neq 0$) in almost all conditions (negative values in the dark conditions $\Delta Y < 0$, and positive in the bright conditions $\Delta Y > 0$).

the chromatic induction mainly depends on the activation of l and Y channels. Nevertheless, significant interactions exist between l and s, $F(2, 265.89) = 18.83$, $p < .0001$, l and Y, $F(4, 265.53) = 8.02$, $p < .0001$, and s and Y channels, $F(8, 265.64) = 2.12$, $p = .0346$.

Therefore, the chromatic induction along the l axis depends on the interaction between all channels.

In a similar fashion, a main effect of ConditionL, $F(2, 238.12) = 12.19$, $p < .0001$, and ConditionY, $F(4, 266.91) = 17.91$, $p < .0001$, have been observed in

the chromatic induction along the *s* axis. In contrast with the previous model, the triple interaction between ConditionL, ConditionS, and ConditionY is also significant, $F(8, 266.44) = 6.57$, $p < .0001$. Again, we can conclude that chromatic induction along the *s* axis depends on the values of the *lsY* channels.

The post hoc analysis of the model along the *l* axis (red line in Figure 2) shows that, although the interaction between ConditionL and ConditionS is significant, color induction effect is similar for the different *s* conditions. That is, the effect do not vary that much from top to bottom rows in left or right columns (e.g., $-l/5$ vs $-l/+s/5$: $t-ratio[274] = -1.49$, $p_{adj} = .3420$; $-l/5$ vs $-l/-s/5$: $t-ratio[274] = 0.91$, $p_{adj} = .6150$). Exceptions occur in $-l/-10$ vs $-l/+s/-10$: $t-ratio[276] = -2.51$, $p_{adj} = .0205$; and $+l/$ [-10] ($+l/$ [-10] vs $+l/+s/-10$: $t-ratio[276] = 3.33$, $p_{adj} = .0023$; $+l/$ [-10] vs $+l/-s/-10$: $t-ratio[276] = -3.31$, $p_{adj} = .0023$), where significant differences were observed. Furthermore, we want to stress that, although striped surrounds were used, several chromatic conditions such as $-l/<0$ and $-l/-s/<0$ induced color contrast instead of color assimilation.

In contrast, the post hoc analysis of the model along the *s* axis reveals that chromatic induction along the *s* axis (purple lines in Figure 2) depends on the *l* condition. That is, the color induction effects varies from left to right panels in top and bottom rows, being the strongest assimilation in $+s/-10$ ($+s/-10$ vs $-l/+s/-10$: $t-ratio[277] = -5.36$, $p_{adj} < .0001$; $+s/-10$ vs $+l/+s/-10$: $t-ratio[277] = 4.59$, $p_{adj} < .0001$), and $-s/10$ ($-s/10$ vs $-l/-s/10$: $t-ratio[277] = -4.45$, $p_{adj} = .0001$; $-s/10$ vs $+l/-s/10$: $t-ratio[277] = 4.40$, $p_{adj} = .0001$). Interestingly, in both cases, the strongest assimilation effect is observed when the *l* channel is not activated, and the effect is dramatically decreased when it is.

Regarding our initial hypothesis, at equiluminance, we never observed color assimilation in neither cardinal nor diagonal conditions. In fact, in this luminance condition we always observed no color induction, except for $-l/0$ where color contrast was induced.

Brightness induction

As reported in Cerda-Company et al. (2018), cardinal conditions ($+l$, $-l$, $+s$, $-s$) not only induced chromatic induction, but they induced a small brightness induction. Let $\Delta B = Y^c - Y^t$ be the luminance difference between the comparison (Y^c) and the test ring (Y^t). In the present study, a brightness induction effect (Figure 3) is present at those points where ΔB differ from zero. For nonequiluminant conditions, a small brightness contrast was observed except for $\Delta Y = 5$ ($\Delta B = 0.1[1.72]$, $V = 1805$, $p = .4978$). In

the test stimulus (Figure 1), the surround formed a luminance uniform annulus, therefore, it is not surprising that the test shifted away from the luminance of the surround (brightness contrast). This can be observed where the test ring is perceived darker in the dark conditions ($\Delta Y = -10$: $\Delta B = -1.49 \pm 0.76$, $t[82] = -17.92$, $p < 2.2e - 16$; and $\Delta Y = -5$: $\Delta B = -1.67 \pm 0.83$, $t[82] = -18.22$, $p < 2.2e - 16$), and brighter in the bright conditions ($\Delta Y = 10$: $\Delta B = 0.86[2.25]$, $V = 2925$, $p = 1.57e - 08$).

Surprisingly, at equiluminance, the test ring is perceived darker ($\Delta B < 0$) than $Y = 20\,\text{cd/m}^2$ ($\Delta B = -0.84[2.28]$, $V = 304$, $p = 7.45e - 10$), but this difference is more enhanced in the diagonal ($\Delta B = -1.66$) than in the cardinal conditions ($\Delta B = -0.13$, $W = 1195$, $p = 6.14e - 06$). Interestingly, only in $+s/0$ and $-s/0$ we do not observe brightness induction at equiluminance.

Discussion

The use of equiluminant stimuli to study color induction is not new. In particular, several authors used them to conclude that the Kirschmann's Third Law (Kirschmann, 1891) rules the color contrast effect (Gordon & Shapley, 2006; Faul et al., 2008; Xing et al., 2015). Although in these studies the authors presented uniform surrounds, color induction effect has also been measured in equiluminant stimuli with striped surrounds (Fach & Sharpe, 1986; Smith et al., 2001; Cerda-Company & Otazu, 2019). Several authors concluded that the spatial frequency of the stripes is a key factor to induce color assimilation (Fach & Sharpe, 1986), and that a transition from color contrast with color assimilation can be produced by doing the stripes thinner and thinner (Smith et al., 2001).

In the present work, we have not studied the effect of the spatial frequency on color assimilation, but we studied the effect of the activated pathways. The effect of luminance on color assimilation has been slightly studied in striped stimuli (De Weert & Spillmann, 1995; Cao & Shevell, 2005; Cerda-Company et al., 2018), and more studied using the watercolor effect (Pinna, 1987; Pinna et al., 2001; Devinck et al., 2005, 2006; Gerardin et al., 2018). De Weert and Spillmann (1995) studied the effect of luminance differences (with an equiluminant condition) on a colored background with red and green inducers. They concluded that the color assimilation depends on the luminance difference (with no color induction at equiluminance), and that this effect also depends on the polarity of this luminance difference, inducing color assimilation when the target was brighter than the inducers. In line with the former observation, several studies observed a weaker color assimilation induced by equiluminant inducers, suggesting that color

assimilation (at least in the Watercolor effect) is the result of a luminance-dependent mechanism (Devinck et al., 2005, 2006; Gerardin et al., 2018). Although our stimuli configuration is significantly different, we also observed no color assimilation at equiluminance, and that the effect depends on the polarity of the luminance difference, with a weak color assimilation in $+l/[>0]$. Similar results were observed by Cao and Shevell (2005). They measured color induction in a wide range of chromatic conditions and in two different luminance conditions (with the target either darker or brighter than the inducers). Our work is similar to the latter one in the sense that the target is always the EEW and we spread the chromaticities of the inducers around the target in the MacLeod–Boynton colorspace. Specifically, because they did not define an equiluminant condition, they evaluated the interaction between two or three pathways. In their study, they observed that the $+s$ and $-s$ conditions are more likely to induce color assimilation or no induction than $+l$ and $-l$ conditions, as observed in our results.

Regarding our initial hypothesis, we expected to observe color assimilation at equiluminance in diagonal conditions ($-l/+s/0$, $+l/+s/0$, $-l/-s/0$ and $+l/-s/0$), when both chromatic K and P pathways were activated. Our results do not support the hypothesis, because the observed color induction is not stronger than the JND. Therefore, the influence of chromatic pathways between each other is not strong enough to induce color assimilation. In fact, color assimilation was only observed in those conditions where the luminance M pathway was activated (e.g., $\Delta C_l > 0$ in $-l/+s/10$ and $+l/-s/10$, and $\Delta C_s > 0$ in $-l/+s/-10$, $+s/-10$, $+l/+s/10$), with the chromatic pathways influencing each other when it was activated (the results depend on the interaction between ConditionL, ConditionS, and ConditionY).

One possible explanation is that a mutual inhibition–like mechanism does not exist between chromatic pathways. Indeed, one possible interpretation could be that they indirectly influence each other through the luminance pathway, that is, a chromatic pathway influences the luminance pathway and this one, in turn, influences the other chromatic pathway. This can be observed in ΔC_s for $+s/-10$ (K pathway), which is dramatically decreased when the P pathway was activated ($-l/+s/-10$ and $+l/+s/-10$ conditions). According to this interpretation, when P pathway was activated ($-l/+s/-10$ or $+l/+s/-10$ conditions) it inhibited the M pathway and, as a consequence, the M pathway could not inhibit as much the K pathway. In contrast, in $+s/-10$, the M pathway could inhibit the K pathway because the P pathway was not inhibiting it.

In addition, we observed different behaviors for the P and K pathways. Although this observation is not new (Cao & Shevell, 2005; Cerda-Company et al., 2018; Cerda-Company & Otazu, 2019), it suggests that the P pathway has more influence on the M pathway and, in

turn, on the K pathway, than vice versa. In that sense, ΔC_l (Figure 2) has less variation from bottom ($-s$) to top ($+s$) conditions than ΔC_s from left ($-l$) to right ($+l$) conditions.

Our interpretation assumes that the site of the effects is cortical (Zaidi et al., 1992; Rossi et al., 1996; De Weert & Kruysbergen, 1997; Zaidi, 1999; Shapley & Hawken, 2002; Cao & Shevell, 2005), but the results in Figure 2 show that color induction is not easy to be explained by low level mechanisms, mainly because the effect does not only depend on the values of l, s or Y, but also on a complex combination of them. As observed in previous studies, color induction occurs along the different color axes (i.e., different angles) of the color space, with selective changes for particular colors: the natural color distributions, and the daylight blue–yellow color axis (Webster et al., 2002; Klauke & Wachtler, 2015). These observations suggest that color induction could be not only a consequence of low-level processes, but also owing to high-level processes. These selective changes are also observed in Figure 2, where $+s$ and $-s$ conditions (which could be considered similar to the daylight blue–yellow color axis) are completely different between each other, and completely different to the rest. In contrast, both $-l/+s$ and $+l/+s$ conditions are similar, but slightly different to $-l/-s$ and $+l/-s$. Furthermore, color contrast ($\Delta C < 0$) is mainly observed in $-l$ condition, which could be approximately related to foliage color. All these selective changes in color induction for particular chromatic conditions could suggest that color induction can be affected by high-level mechanisms. Whether the influence could be through a top–down feedback influence or through some neural mechanisms present in higher level areas is an open question.

The results in Figure 3 show that chromatic information in the surround area influences the brightness perception of the test ring. That is, chromatic variation in the surround can induce brightness induction. This finding goes inline with Lotto and Purves (1999), who showed that multicolored chromatic surrounds generate stronger brightness induction than uniform ones. Interestingly, we observed that, at equiluminance, no brightness induction is induced when the P pathway is not activated ($+s$ and $-s$ conditions). Furthermore, not only the chromatic variability of the inducers influences the brightness induction, but also the luminance difference between the target and the first inducer (the ΔY). In a previous experiment, Hong and Shevell (2004) concluded that the luminance context influences the brightness induction on the target region. If ΔY did not affect the brightness induction, we would observe a diagonal distribution in Figure 3, with a shift owing to the influence of chromatic variability (Lotto & Purves, 1999). Hence, because we observe that shifting for the $-l$ and $+l$ conditions, we conclude that the degree of brightness induction depends on both the chromatic variability of the surround and

the luminance difference between the target and the surround.

The brightness induction (ΔB in Figure 3) is different in $+s/0$ compared with both $-l/+s/0$ and $+l/+s/0$, suggesting that the P pathway (when activated) modifies the activity of M pathway. This observation could support the possibility that the activation of the P pathway could influence the M pathway and this, in turn, could modify the response of the K pathway. But, if the P pathway simply inhibited or enhanced M pathway, we would have observed a change in the slope of the curve. Because we do not observe a slope change but a shifting, we cannot conclude that the P pathway either enhances or inhibits the M pathway (which depends on the signs of both ΔB and ΔY). Nonetheless, a clear influence of P over M pathway is observed. This influence is a reduction (negative shifting) of the absolute value of the brightness. Hence, to clarify the real nature of the influence of P on M pathway, a more detailed, future study would be necessary.

Some properties of visual stimuli used in this study are not comparable with some previous studies. For example, Shevell and Monnier (2005) showed that chromatic assimilation is maximum for rings of a spatial frequency equal to 3.3 cpd. Because the aim of the present study is the comparison of the new diagonal conditions against the existing cardinal ones (Cerda-Company et al., 2018), we have used the same visual stimuli ($\sim$ 2 cpd). Considering the objective of the present study, we need a stimuli that are able to generate either assimilation or contrast just by changing the luminance of the test ring and/or the chromaticities of the inducers. Hence, although a spatial frequency of 3.3 cpd could induce stronger assimilation effect, it is not clear whether it would induce a chromatic contrast effect. Another property is that our stimuli do not have the same number of inducers at every side of the test ring. Our designed considered four and six inducer rings at each side. Because previous studies used four rings at each side (Monnier & Shevell, 2003, 2004; Shevell & Monnier, 2005), we consider that the effect of them on the results is negligible.

As a future work, it would be interesting to study whether the brightness induction effect observed in our results is due to the brightness differences produced by the equiluminant stimuli or by the chromatic variation of the inducers. We know that equiluminant stimuli could have brightness differences, and equibrightness stimuli could have luminance differences. Therefore, conducting similar experiments, but using equibrightness instead of equiluminant stimuli, could explain the origin of this effect. If chromatic variation accounts for the brightness induction, both equiluminant and equibrightness stimuli would show brightness induction. In contrast, if brightness (but not luminance) differences accounts for this effect, the brightness induction would be negligible.

Conclusions

From the results presented here, we can conclude that both luminance and chromatic conditions influence the color assimilation effect, being the luminance differences a key factor. Indeed, we hypothesized that activating both chromatic pathways (and deactivating the luminance one), we would find color assimilation, if a mutual inhibition–like mechanism exist between the chromatic pathways. Our results do not support this hypothesis; therefore, it is unlikely to suggest the existence of a mutual inhibition–like mechanism between chromatic pathways. Nevertheless, our results suggest that chromatic pathways influence each other through the luminance pathway. When all the visual pathways are activated, a chromatic pathway influences the luminance one through the mutual inhibition mechanism and, in turn, the latter pathway influences the other chromatic one through the mutual inhibition mechanism. Furthermore, it seems that the influence of the parvo- on the koniocellular pathway, through the magnocellular pathway, is stronger than the opposite, and that color assimilation is stronger along the s than along the l chromatic axes of the MacLeod–Boynton colorspace.

In our results, we observed a small brightness induction effect that could be explained by the chromatic variations of the inducers, but as discussed before, more future work in this direction would be interesting.

Keywords: color vision, color assimilation, color induction, psychophysics, mutual inhibition

Acknowledgments

Commercial relationships: none.
Corresponding author: Xavier Otazu.
Email: xotazu@cvc.uab.cat.
Address: Computer Vision Center and Computer Science Department, Edifici O, Campus UAB, Cerdanyola del Valles (Bellaterra), 08193 Barcelona, Spain.

References

Bimler, D. L., Paramei, G. V., & Izmailov, C. A. (2009). Hue and saturation shifts from spatially induced blackness. *Journal of the Optical Society of America A, 26*(1), 163–172.

Boynton, R. M. (1973). Implications of the minimally distinct border. *Journal of the Optical Society of America, 63*(9), 1037–1043.

Boynton, R. M., & Kaiser, P. K. (1968). Vision: The additivity law made to work for heterochromatic photometry with bipartite fields. *Science, 161*(3839), 366–368.

Brill, M. H. (2014). Minimally distinct border. In M. R. Luo (Ed.), *Encyclopedia of color science and technology* (pp. 1–3). Berlin, Heidelberg: Springer Berlin Heidelberg.

Cao, D., & Shevell, S. K. (2005). Chromatic assimilation: spread light or neural mechanism? *Vision Research, 45*(8), 1031–1045.

Cerda-Company, X., & Otazu, X. (2019, Jan). Color induction in equiluminant flashed stimuli. *Journal of the Optical Society of America. A, Optics, Image Science, and Vision, 36*(1), 22.

Cerda-Company, X., Otazu, X., Sallent, N., & Parraga, C. (2018, 10). The effect of luminance differences on color assimilation. *Journal of Vision, 18*(11), 10.

Chevreul, M. E. (1839). *De la loi du contraste simultane des couleurs*. Paris: Chez Pitois-Levrault et Ce.

De Weert, C. M., & Kruysbergen, N. A. (1997). Assimilation: central and periferal effects. *Perception, 26*(10), 1217–1224.

De Weert, C. M., & Spillmann, L. (1995). Assimilation: Asymmetry between brightness and darkness? *Vision Research, 35*(10), 1413–1419.

Devinck, F., Delahunt, P. B., Hardy, J. L., Spillmann, L., & Werner, J. S. (2005). The watercolor effect: Quantitative evidence for luminance-dependent mechanisms of long-range color assimilation. *Vision Research, 45*, 1413–1424.

Devinck, F., Spillmann, L., & Werner, J. S. (2006). Spatial profile of contours inducing long-range color assimilation. *Visual Neuroscience, 23*, 573–577.

Ehrenstein, W. (1941). Ber abwandlungen der l. Hermannschen helligkeitserscheinung. *Zeitschrift fur Psychologie, 150*, 83–91.

Fach, C., & Sharpe, L. T. (1986). Assimilative hue shifts in color gratings depend on bar width. *Perception & Psychophysics, 40*(6), 412–418.

Farnsworth, D. (1947). *The farnsworth dichotomous test for color blindness: panel d-15 [Computer software manual]*. Psychological Corporation.

Faul, F., Ekroll, V., & Wendt, G. (2008). Color appearance: The limited role of chromatic surround variance in the 'gamut expansion effect'. *Journal of Vision, 8*(30), 1–20.

Gerardin, P., Dojat, M., Knoblauch, K., & Devinck, F. (2018). Effects of background and contour luminance on the hue and brightness of the watercolor effect. *Vision Research, 144*, 9–19.

Gordon, J., & Shapley, R. (2006). Brightness contrast inhibits color induction: Evidence for a new kind of color theory. *Spatial Vision, 19*, 133–146.

Hong, S. W., & Shevell, S. K. (2004). Brightness contrast and assimilation from patterned inducing backgrounds. *Vision Research, 44*(1), 35–43.

Ishihara, S. (1972). *Tests for colour-blindness*. Tokyo, Japan: Kanehara Shippan Co., Ltd.

Johnson, E. N., Hawken, M. J., & Shapley, R. (2001). The spatial transformation of color in the primary visual cortex of the macaque monkey. *Nature Neuroscience, 4*(4), 409–416.

Johnson, E. N., Hawken, M. J., & Shapley, R. (2008). The orientation selectivity of color-responsive neurons in macaque v1. *Journal of Neuroscience, 28*(32), 8096–8106.

Kaiser, P. (1971). Minimally distinct border as a preferred psychophysical criterion in visual heterochromatic photometry. *Journal of the Optical Society of America A, 61*(7), 966–971.

Kaiser, P., Lee, B., Martin, P., & Valberg, A. (1990). The physiological basis of the minimally distinct border demonstrated in the ganglion cells of the macaque retina. *Journal of Physiology, 422*, 153–183.

Kaneko, S., & Murakami, I. (2012). Flashed stimulation produces strong simultaneous brightness and color contrast. *Journal of Vision, 12*(1), 1–18.

Kenward, M. G., & Roger, J. H. (1997). Small sample inference for fixed effects from restricted maximum likelihood. *Biometrics, 53*(3), 983–997.

Kirschmann, A. (1891). Ueber die quantitativen verhaltnisse des simultanen helligkeits- und farben-contrastes. *Philosophische Studien, 6*, 417–491.

Klauke, S., & Wachtler, T. (2015, 09). Tilt in color space: Hue changes induced by chromatic surrounds. *Journal of Vision, 15*(13), 17–17.

Lotto, R., & Purves, D. (1999). The effects of color on brightness. *Nature Neuroscience, 2*(11), 1010–1014.

MacLeod, D. A., & Boynton, R. M. (1979). Chromaticity diagram showing cone excitation by stimuli of equal luminance. *Journal of the Optical Society of America, 69*(8), 1183–1186.

Monnier, P., & Shevell, S. K. (2003). Large shifts in color appearance from patterned chromatic backgrounds. *Nature Neuroscience, 6*, 801–802.

Monnier, P., & Shevell, S. K. (2004). Chromatic induction from s-cone patterns. *Vision Research, 44*, 849–856.

Nunez, V., Shapley, R. M., & Gordon, J. (2018). Cortical double-opponent cells in color perception: Perceptual scaling and chromatic visual evoked potentials. *i-Perception, 9*(1), 1–16.

Otazu, X., Parraga, C. A., & Vanrell, M. (2010). Toward a unified chromatic induction model. *Journal of Vision, 10*(12), 1–24.

Pinna, B. (1987). Un effetto di colorazione. In: V. Majer, M. Maeran, & M. Santinello (Eds.), *Il laboratorio e la città. XXI Congresso degli Psicologi Italiani* (pp. 1–58). Milano: Società Italiana di Psicologia.

Pinna, B., Brelstaff, G., & Spillmann, L. (2001). Surface color from boundaries: A new 'watercolor' illusion. *Vision Research, 41*, 2669–2676.

R Core Team. (2019). *R: A language and environment for statistical computing [Computer software manual]*. Vienna, Austria. Available: https://www.R-project.org/.

Rossi, A. F., Rittenhouse, C. D., & Paradiso, M. A. (1996). The representation of brightness in primary visual cortex. *Science, 273*(5278), 1104–1107.

Shapley, R., & Hawken, M. J. (2002). Neural mechanisms for color perception in the primary visual cortex. *Current Opinion in Neurobiology, 12*(4), 426–432.

Shapley, R., & Hawken, M. J. (2011). Color in the cortex: single- and double-opponent cells. *Vision Research, 51*(7), 701–717.

Shevell, S. K., & Monnier, P. (2005). Color shifts from s-cone patterned backgrounds: Contrast sensitivity and spatial frequency selectivity. *Vision Research, 45*(9), 1147–1154.

Smith, V. C., Jin, P. Q., & Pokorny, J. (2001). The role of spatial frequency in color induction. *Vision Research, 41*(8), 1007–1021.

Smith, V. C., & Pokorny, J. (1975). Spectral sensitivity of the foveal cone photopigments between 400 and 500 nm. *Vision Research, 15*, 161–171.

Van Tuijl, H. F. J. M. (1975). A new visual illusion: neonlike color spreading and complementary color induction between subjective contours. *Acta Psychologica, 39*, 441–445.

Von Bezold, W. (1876). *The theory of color and its relation to art and art-industry*. Boston: L. Prang and Company.

Wagner, G., & Boynton, R. (1972). Comparison of four methods of heterochromatic photometry. *Journal of Optical Society of America A, 62*(12), 1508–1515.

Webster, M. A., Malkoc, G., Bilson, A. C., & Webster, S. M. (2002, 11). Color contrast and contextual influences on color appearance. *Journal of Vision, 2*(6), 7–7, https://doi.org/10.1167/2.6.7, [Article]

Xing, D., Ouni, A., Chen, S., Sahmoud, H., Gordon, J., & Shapley, R. (2015). Brightness-color interactions in human early visual cortex. *Journal of Neuroscience, 35*(5), 2226–2232.

Zaidi, Q. (1999). Color and brightness induction: from mach bands to three-dimensional configurations. In K. R. Gegenfurtner, & L. T. Sharpe (Eds.), *Color vision: From genes to perception* (pp. 317–344). Cambridge, UK: Cambridge University Press.

Zaidi, Q., Yoshimi, B., Flanigan, N., & Casanova, A. (1992). Lateral interactions within color mechanism in simultaneous induced contrast. *Vision Research, 32*(9), 1695–1707.
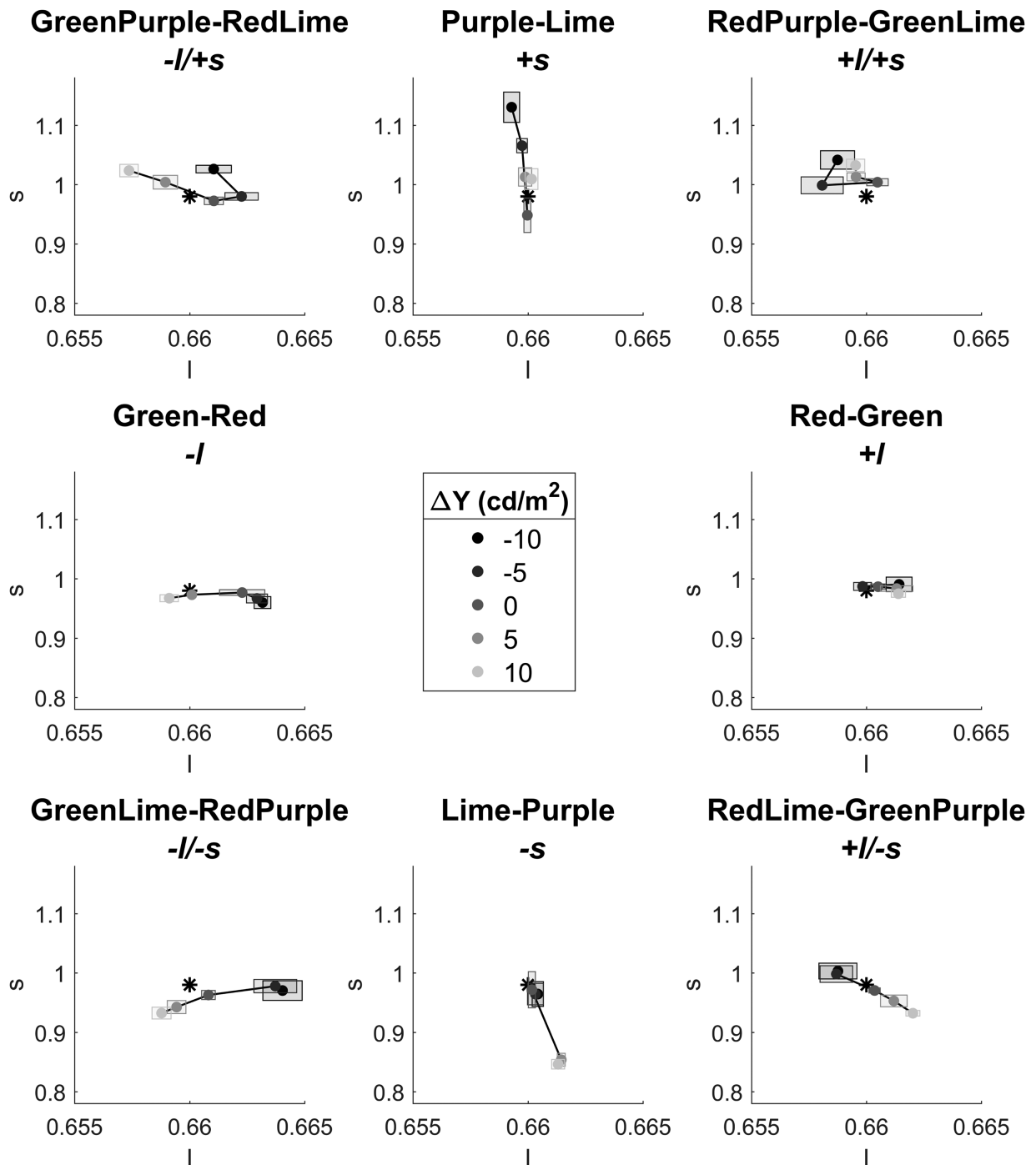
Appendix A: Results in MacLeod–Boynton space

Figure 4. Same results as in Figure 2, but shown in the MacLeod–Boynton color space. Error boxes are standard error of means. Achromatic EEW is shown as an asterisk.
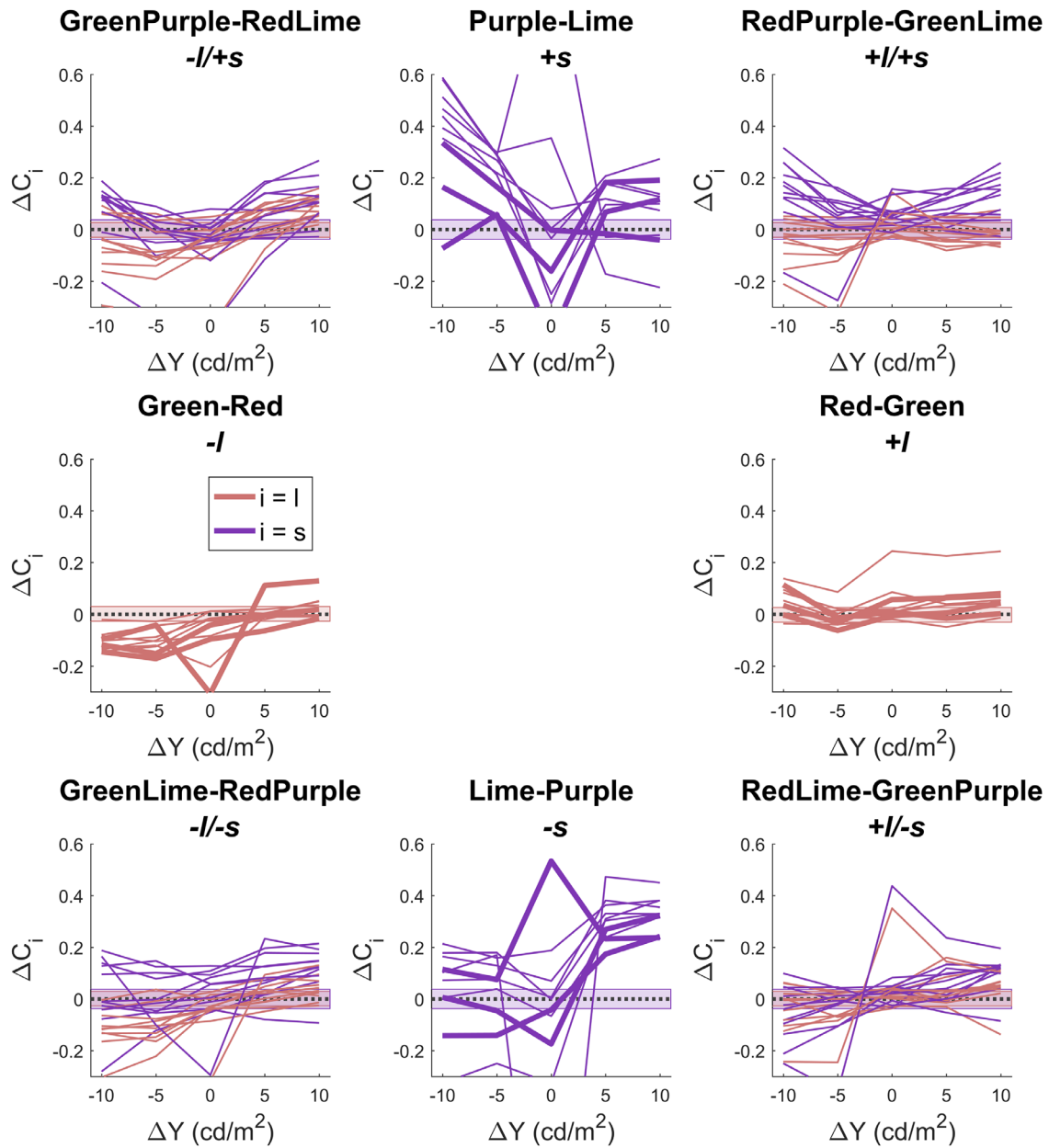
Appendix B: Individual results

Figure 5. Individual results on all the defined conditions. Data on cardinal axis (e.g., *+l, −l, +s, −s,*) are extended from Cerda-Company et al. (2018) (new participants are indicated by thick lines), and results on the diagonal axis (e.g., *+l/+s, +l/−s, −l/+s, −l/−s*) have been obtained in the present study.

Appendix C: Statistical models

	Type III analysis of variance table with Kenward–Roger's method Color induction$_l$					
	Mean Sq	NumDF	DenDF	F-value	*p* value	signif.
ConditionL	0.1160	1	265.91	33.12	2.38e-08	***
ConditionS	0.0013	2	231.47	0.38	.6856	
ConditionY	0.1385	4	265.76	39.56	<2.2e-16	***
ConditionL:ConditionS	0.0659	2	265.89	18.83	2.26e-08	***
ConditionL:ConditionY	0.0281	4	265.53	8.02	4.03e-06	***
ConditionS:ConditionY	0.0074	8	265.64	2.12	.0346	*
ConditionL:ConditionS:ConditionY	0.0050	8	265.53	1.43	.1827	
	Color induction$_s$					
	Mean Sq	NumDF	DenDF	F-value	*p* value	Signif.
ConditionL	0.1347	2	238.12	12.19	9.085e-06	***
ConditionS	0.0243	1	266.42	2.20	.1394	
ConditionY	0.1977	4	266.91	17.91	4.847e-13	***
ConditionL:ConditionS	0.0637	2	266.57	5.77	.0035	**
ConditionL:ConditionY	0.0421	8	266.76	3.81	.0003	***
ConditionS:ConditionY	0.2616	4	266.48	23.70	<2.2e-16	***
ConditionL:ConditionS:ConditionY	0.0725	8	266.44	6.57	7.958e-08	***

Signif. codes: 0 '***', 0.001 '**', 0.01 '*', 0.05 ' '

Table 2. Statistical details of color induction linear models with mixed effects.